

Drillability predictions in Aravalli and Himalayan rocks – a petro-physico-mechanical approach

B. N. V. Siva Prasad^{1,*}, V. M. S. R. Murthy² and Sripad R. Naik¹

¹Numerical Modelling Department, National Institute of Rock Mechanics, Bengaluru 560 070, India

²Department of Mining Engineering, Indian Institute of Technology (Indian School of Mines), Dhanbad 826 004, India

Dolomite, siliceous dolomite, phyllite, schist, leucogranite, pegmatite and gneissic rocks from the Indian Aravalli Hills and Bhutan Himalayan mountains were studied to examine the influence of petrographic and physico-mechanical properties on rock drillability. From petrographic assessments, a measure of grain size distribution, i.e. ‘granularity index’ and a ‘modified saturation index’ are proposed. Extensive rock mechanics and drilling experiments were also performed to correlate physico-mechanical properties with intact rock drillability. Statistical analysis revealed that no single petrographic parameter could completely explain the variance in drill penetration rate (DPR). The proposed indices and the petro-physico-mechanical approach helped in the rapid assessment of DPR in hard rocks.

Keywords: Granularity index, hard rock drillability, modified saturation index, petrography, physico-mechanical approach.

ROCK drillability, also known as drill penetration rate (DPR), is a measure of advancement of drill bit or tool into the rock in unit time, usually measured in millimetres per minute. DPR is an important measure in all excavation projects in various sectors like mining, tunnelling, hydropower, caverns, crude oil storage, nuclear, infrastructure and lately other planetary bodies too. Drill and blast (D&B) technology is the prominent method used to excavate materials in hard rocks due to its ease of adaptability¹. An accurate assessment of rock drillability helps the project planners, financiers and the executing engineers to plan for deployment of suitable equipment to drill through a given geotechnical environment and accordingly manage the drilling inventory which aids in planning the progress of the project. Thus, it is of utmost importance to understand the influential parameters that affect rock drillability. Over the years researchers have attempted to study various parameters influencing rock drillability helping the industry to a certain extent, but could not aid in the precise prediction of DPR due to the inherent complexities of rock^{2–17}.

Rock is an assemblage of minerals, while a mineral is a naturally occurring inorganic chemical compound with an established crystal structure. The rocks are identified depending on the relative mineral abundance and their textural relationships. Minerals can be described by size, shape and habit of the crystal, its colour, presence of cleavages, refractive index, interference colour, extinction angle and twinning or zoning of crystals¹⁸. The type of mineral assemblage, texture and hardness contribute to strength-deformation characteristics of rock, while the presence of microcavities greatly controls the mechanical behaviour of rocks¹⁹. The microstructure of rocks provides resistance to inter- or intragranular crack propagation^{20,21}, and can be correlated with rock strength and drillability parameters. These petro-physico-mechanical (PPM) properties influence drillability at the micro level²². Hence the presence of various mineral grains, their modal volume percentage, arrangement in the matrix, percentage of essential and non-essential minerals and their inter-relationships will provide an insight into the overall strength, deformation, abrasion, hardness and drillability characteristics of the rocks.

Extensive drilling and blasting activities are accomplished to facilitate rock excavation in both mining and hydroelectric sectors. The Aravalli ranges being mineral-rich (lead–zinc) is an active hard-rock mining province in India, while the Bhutan Himalayan mountain valleys accommodate gigantic powerhouse caverns of hydroelectric projects. Excavations in these sectors demand huge meterage of drilling through hard, abrasive, meta-sedimentary and igneous rocks, shear zones and intrusions prevailing under complex geotechnical setups. Rocks found in these terrains are most commonly dealt with in underground hard-rock excavations. The aim of the present study is to understand the influence of various rock types on rock drillability comprehensively having diversified petrographic and physicomachanical properties and to facilitate the subsequent excavation processes such as blasting and supporting.

While drilling, stress is built up under the indenting tool during the bit–rock interaction process and rock behaviour under the impact-generated stress depends on its physico-mechanical properties and the method of drilling.

*For correspondence. (e-mail: sivaprasadbnv@yahoo.in)

Rock breakage in percussion can be classified into four phases, viz. crushed zone, crack formation, crack propagation and chipping²³. To drill through rock, the drill bit must overcome the surface hardness followed by the strength of the rock, thereby crushing the mineral grains in the drill bit trajectory. Indentation only occurs when the induced stress beneath the drill bit exceeds the inherent strength of the rock. Over years of research, several rock properties like density, porosity, compressive and tensile strength, ultrasonic velocity, Young's modulus, Poisson's ratio, cohesion, friction angle, abrasivity and hardness were found to influence rock drillability to varying extents. However, their relationships with the PPM properties vis-à-vis rock drillability in the Aravalli Hills and Bhutan Himalayan hard rocks have not been reported.

Thus, the present study aims to explore the underlying constructs between petrographic, physico-mechanical and drillability properties of hard rocks originating from these terrains and determine the most influential parameters affecting rock drillability. Here, drillability was assessed in the rocks originated from the Aravalli Hills in the western part of India to Himalayan mountains in the Royal Kingdom of Bhutan. Such relationships greatly help the drill bit and equipment manufacturers to develop an optimum configuration resulting in better penetration rates for a given geotechnical environment.

Geology

The locations selected for the present study comprise of Zawar group of mines from the Aravalli ranges, Rajasthan, India, and Punatsangchhu-II Hydroelectric Project (PHEP-II) from Himalayan mountains, Bhutan. Zawar rocks form a part of the Aravalli Supergroup from the Palaeoproterozoic (2400–1700 Ma)^{24,25}, which is the oldest fold mountain range in India²⁶. Metasedimentary rocks belonging to the Aravalli Supergroup overlie a basement exposed south of Zawar, which is a polyphase, deformed, complexly folded geological structure formed out of two distinct epochs of post-Aravalli and post-Delhi orogenies. The rock units consist of dolomite, greywacke, sub-greywacke and phyllite/quartzite.

PHEP-II is located within a part of the Tethyan Belt, central crystalline of Thimphu Group from the Precambrian (~541 Ma)²⁷. The exposures are generally found to be competent with the presence of coarse-grained, quartzofeldspathic, biotite–muscovite and bands of mica schist, quartzite and concordant veins of foliated leucogranite, migmatites with minor metabasic rocks belonging to Sure and Chekha formations of the Precambrian and leucogranite of Late Miocene–Pleistocene. The main rock types exposed in the project area include quartzofeldspathic gneisses, banded gneisses, biotite gneisses/schist with quartzite bands, leucogranite and pegmatite. Gneissic rocks comprise of augen, rich biotite, medium to coarse-

grained granite, leucocratic and contain quartz feldspar besides biotite with sub-ordinate muscovite and garnet as a mineral assemblage. Figure 1 depicts the geological setup of the study locations from India and Bhutan^{28,29}. The age of the rocks indicates details such as genesis, temperature, confining pressure, rock type, structure, intrusions and time of formation which have an impact on the strength and deformability of the rocks. The Aravalli ranges from the Palaeoproterozoic and Bhutan Himalayan rocks from the Precambrian considered in this study have a huge geological age gap between them. Leaching or metasomatism and weathering also impact the strength of the rocks irrespective of the age of formation. Thus, their associated rock properties are expected to vary which in turn will have a significant influence on rock drillability. This calls for in-depth research to examine the causes, thus helping assess the drillability of rocks and aid in drill selection.

Design of experiments

The present study covers rock types that are most commonly encountered and difficult to deal with in underground, hard-rock mines and hydroelectric projects that are hard and abrasive. Rock samples were collected from underground mines of Zawar, HZL (Aravalli Hills) and underground tunnels and caverns of PHEP-II (Himalayan mountains). The samples were brought to the laboratories of the Indian Institute of Technology (Indian School of Mines) (IIT(ISM)), Dhanbad and National Institute of Rock Mechanics (NIRM), Bengaluru. Block samples were cored and machined to meet various test standard requirements. It was ensured that the tested cored specimens are free from any mega-scale visible defects. Rock mechanics tests were performed on these specimens to determine the physico-mechanical and drillability properties. After testing, the rock specimens were cut along the drilling direction and thin sections were prepared for further petrographic assessment. The rock variants covered in this study include dolomite (Dol), siliceous dolomite (SD), siliceous phyllitic dolomite (SPD), phyllite (Phy), quartz mica schist (QMS), schist (Sch), leucogranite (Lg), pegmatite (Pg), quartz biotite gneiss (QBG) and mica schist (MS).

Laboratory testing

Physico-mechanical properties

Physico-mechanical properties indicate that the response of rocks to a particular loading type in the drilling process is of utmost importance to understand its impact on drillability^{30–32}. Previous studies in this field have indicated that several parameters influence rock drillability. Rock mechanics tests were performed conforming to

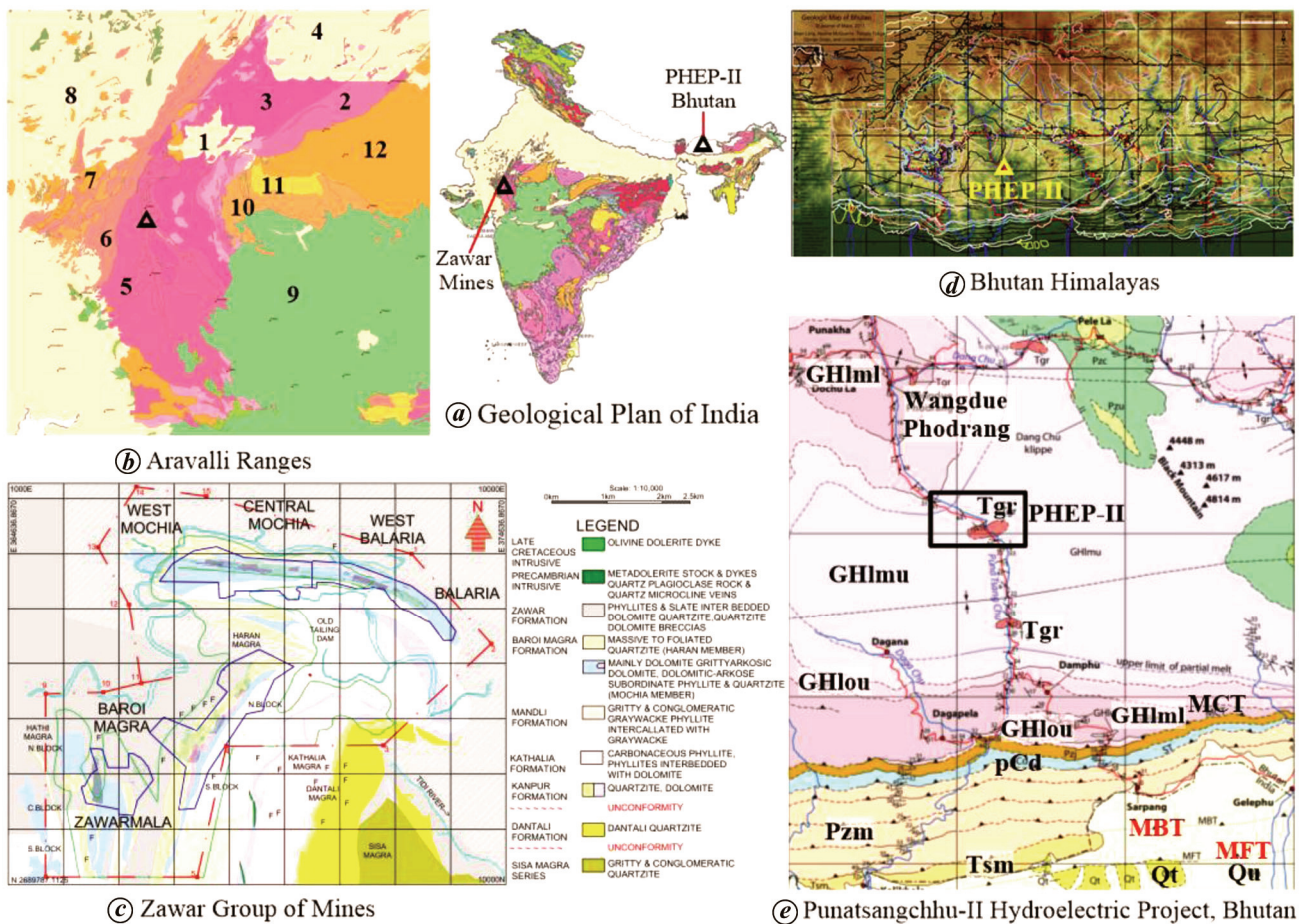


Figure 1. Geological set-up of the study areas from India and Bhutan. 1, Fine aeolian sand and silt with occasional kankar; 2, Archaean – Bhilwara, phyllite; 3, Archaean – Bhilwara composite gneiss and migmatite; 4, Quaternary, fine sand, silt and clay; 5, Palaeoproterozoic, phyllite, chlorite schist; 6, Palaeoproterozoic – mesoproterozoic, quartzite; 7, Neoproterozoic, medium grained granite; 8, Holocene, fine aeolian sand and silt with occasional kankar; 9, Late cretaceous – palaeocene, basalt; 10, Mesoproterozoic sandstone; 11, Mesoproterozoic – neoproterozoic, quartzitic sandstone with conglomerate and shale; 12, Neoproterozoic, shale with limestone bands; GHlmu, Upper metasedimentary unit (Neoproterozoic–Ordovician); GHlou, Orthogneiss unit (Cambrian–Ordovician); GHlml, Lower metasedimentary unit (Neoproterozoic–Cambrian); Tgr, Leucogranite (Miocene) – massive to foliated; Qt, River terraces; Qu, Undifferentiated and unconsolidated sediments deposited in braided stream; Pzm, Manas formation (Neoproterozoic–Cambrian); pCd, Daling formation.

international standards on machined rock specimens to determine the influential rock parameters such as rock density (ρ), ultrasonic velocities (V_p and V_s), fracture toughness (K_{IC}), Cerchar abrasivity index (CAI), Cerchar hardness index (CHI), brittleness index (S20), drilling rate index (DRI), Brazilian tensile strength (BTS), uniaxial compressive strength (UCS), Young's modulus (E), Poisson's ratio (ν), cohesion (C), friction angle (ϕ), porosity (n), and DPR.

Petrographic properties

Over the years, researchers have noted inter-relationships between physico-mechanical properties and structural, textural, mineralogical and petrological features of rocks^{21,33–42}. The petrographic properties influencing drilling rate are mineralogy, grain shape and size, packing

density, texture, grain orientation, degree of interlocking, quartz content, porosity and grain boundaries^{13,20–22,37,38,43–47}. During drilling, the rock has the least resistance with the presence of weaker or lower hardness minerals, cleavages, fissures, microfractures, non-uniformity in grain size and structural defects in failure zones. Rock texture measures the degree of crystallinity, grain size or granularity, and the fabric or geometrical relationships between the constituents of a rock⁴⁸. Detailed analysis of minerals by optical mineralogy in thin sections and identification of microtexture and structure are critical to understanding the origin, strength of the rock and its associated drillability conditions. This analysis thus includes a basic petrographic description, including visual estimation of grain size, sorting, mineral abundances, fabric and rock classification. In the present study, petrographic analysis was performed adopting three major steps, viz. preparation

of thin sections, digital imaging and petrographic assessment.

Preparation of thin sections: The rock core specimens were used to prepare thin sections along the drilling direction using a LAPRO slab saw conforming to ISRM standards after laboratory drilling tests⁴⁹. This was done to identify the minerals that the drill bit had encountered during laboratory drilling tests and explore the influence of various mineral grains, their orientation, structure, angle between the foliation plane and the drilling direction on the performance of the drill system. Figure 2 shows a schematic layout and sectional view of the drilled core specimen used for the preparation of the thin section.

Digital imaging: ‘Digital imaging’ or ‘digital image acquisition’ is a comprehensive term used for the representation of the visual characteristics of an object, such as mineral grains in a thin section. This step includes processing, compression, storage and display of such images for the next step of petrographic analysis. An Olympus polarizing microscope with an in-built digital camera was used to capture the image of mineral grains from thin sections at various scales (500 and 200 μm).

Petrographic assessment: This refers to the identification and quantification of microscopic features of the rock like mineralogy, texture, grain size distribution, etc. Petrographic analysis is a complex process; however, with the advancement of technology, both in terms of digital imaging and computation, the process has become rapid⁵⁰⁻⁵⁴. In the present study, 28 thin sections were prepared from the samples of drilling experiments and analysed under an Olympus polarizing microscope. Figure 3 shows the petrographic assessment procedure (PAP) adopted in the present study.

The acquired image was processed to determine grain size distribution parameters using WIPFRAG software⁵⁵, while the geometrical features were determined from digitized thin sections. Values of number of grains measured, coverage, sphericity, Rosin Rammler’s uniformity coefficient (N), characteristic grain size (X_c) and Swebrec

undulation coefficient (B) were obtained using the WIPFRAG software. Other geometrical features like grain size, shape, area, perimeter, average Feret’s length and breadth, form factor, aspect ratio, elongation and orientation were computed from digitized thin sections. Mineralogical composition in various thin sections was considered to identify both essential and non-essential minerals. However, to correlate with drillability properties, only essential minerals like quartz, dolomite/carbonate/calcite, feldspar and mica were considered. From the acquired images and subsequent petrographic assessments, various indices such as index of interlocking (g), grain size homogeneity (t)⁵⁶ and texture coefficient (TC)²¹ were computed.

Saturation index (IS) considers only quartz and feldspar contents for hard igneous rocks⁵⁶. Since the rocks studied include predominantly carbonates, calcite mineral percentage was also considered and a modified saturation index (MIS) has been proposed (eq. (1)). Granularity index (GI) is a measure of characteristic grain size of rocks (eq. (2)).

Table 1 presents the computation methodology for GI

$$MIS = \frac{Qz\%}{(Qz + Cal + Fsp)} \times 100, \tag{1}$$

where Qz is quartz, Cal is calcite/dolomite/carbonate and Fsp is feldspar content respectively.

$$GI = \sum_1^{25} c, \tag{2}$$

where c is the cumulative of ‘greater than a particular grain size’, represented by column (c) in Table 1.

Results

Experiments were performed on various rock types to determine the physico-mechanical properties, hardness, abrasivity, drillability and petrographic characteristics of the rocks. All the drilling experiments were performed under controlled conditions maintaining constant machine parameters to explore the influence of rock properties and petrographic features on drillability exclusively. Exploratory, correlational and statistical analysis was performed to understand the relationships between the parameters⁵⁷. Figure 4 shows significant variation in DPR vis-à-vis change in PPM properties. The statistics indicate that wide coverage of rock variants providing sufficient variability in petrography, physico-mechanical properties and drilling parameters has been considered in this study that resulted in varied DPR between 0.3 and 16.8 mm/min. This signifies the relationships between various rock type, their properties and drillability, which require to be mapped.

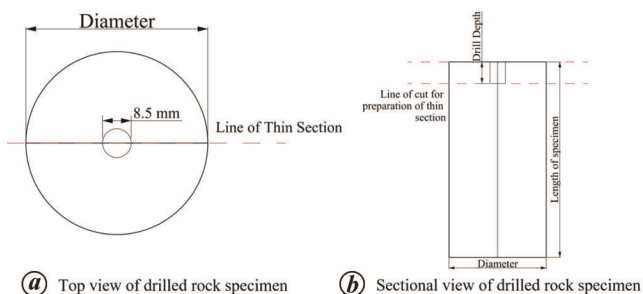


Figure 2. Schematic layout and section of drilled core specimen used for preparation of thin section.

Table 1. Computational procedure for granularity index

Grain size (mm)	Passing or less than grain size (%) (a)	Greater than grain size (%) (b)	Cumulative of (b) (%) (c)	Cumulative number
1.25	100.00	0.00	0.00	c1
1.20	100.00	0.00	0.00	c2
.
0.25	98.82	1.18	1.18	c20
0.20	97.69	1.13	2.31	c21
0.15	91.98	5.71	8.02	c22
0.10	71.23	20.75	28.77	c23
0.05	20.93	50.3	79.07	c24
0.00	0.00	20.93	100.00	c25
		Granularity index	219.35	

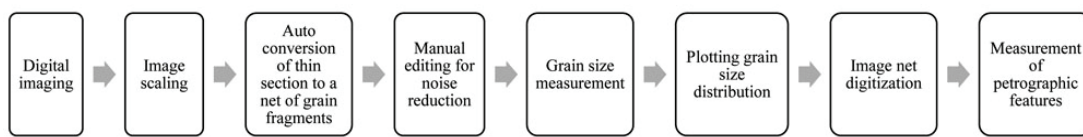


Figure 3. Petrographic assessment procedure.

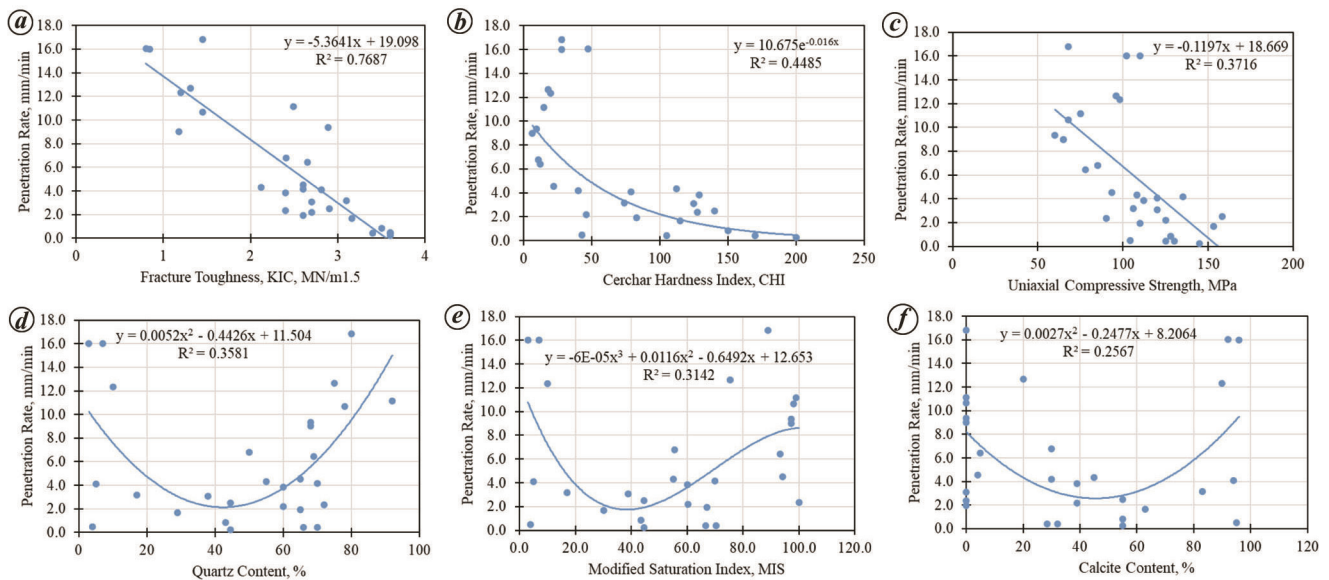


Figure 4. Variation of drill penetration rate (DPR) with change in petro-physico-mechanical (PPM) properties. *a*, PR and K_{IC} ; *b*, PR and CHI; *c*, PR and UCS; *d*, PR and QC; *e*, PR and MIS; *f*, PR and CC.

GI gives a fair idea on relative grain size distribution within the rocks being studied and is calculated from details of grain size acquired using WIPFRAG, that reduces the time required for evaluation of granularity. Lower GI value indicates the presence of a greater percentage of small-sized grains in the thin section and vice versa. Digitized thin sections of two extreme rock specimens with different GI values were studied (Figure 5). Figure 5 *a* and *b* shows thin sections of dolomite and pegmatite rocks considered in this study. Dolomite rock belongs to

the Aravalli Hills from the Archean with a low GI value of 126, while pegmatite rocks belongs to the Bhutan Higher Himalaya from the Precambrian with a higher GI value of 1365 (Figure 5 *c* and *d* respectively). Figure 6 shows grain size distribution curves for both these samples. Figure 6 *a* and *b* show distribution curves of low and high GI specimens, i.e. with 96.91% of less than 0.1 mm (well sorted or homogeneous) and 89.35% of less than 1.15 mm (poor sorting), for dolomite and pegmatite rocks respectively. Figure 7 shows the penetration–time

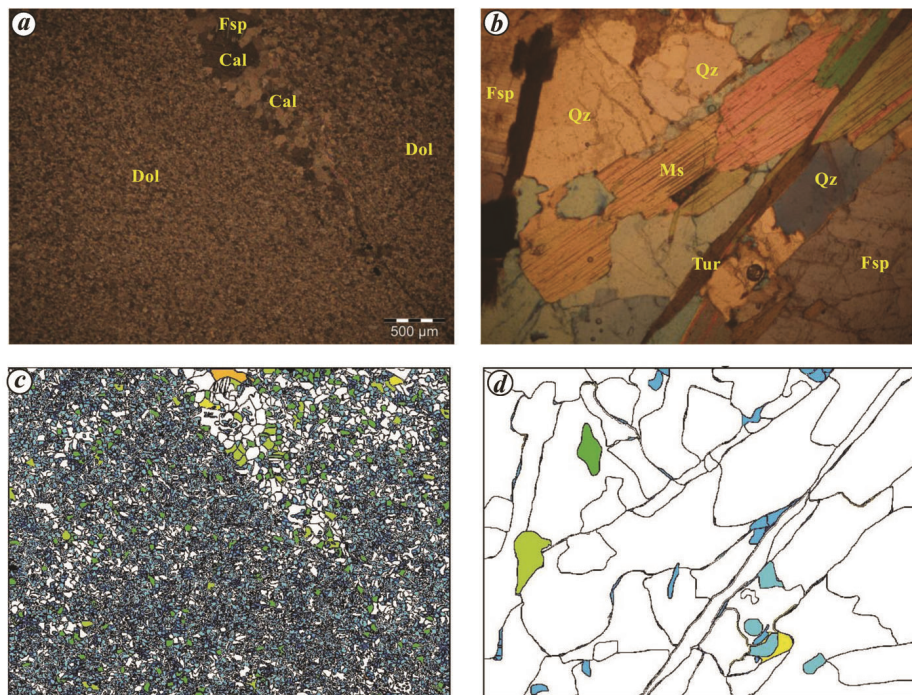


Figure 5. Granularity index (GI) of different rock samples. *a*, Dolomite; *b*, Pegmatite; *c*, GI = 126, DPR = 16 mm/min; *d*, GI = 1365, DPR = 3.1 mm/min. Dol, Dolomite; Fsp, Feldspar; Cal, Calcite; Qz, Quartz; Ms, Muscovite; Tur, Tourmaline.

(*P-T*) curves obtained from drilling tests for these samples.

From Figure 7, it can be observed that the drilling rate in pegmatite is lower than that in dolomite. Under constant drilling conditions, yield stress increases with a decrease in grain size^{33,36,37}, i.e. smaller grains indicate a higher strength and thus low drillability, provided the mineral composition remains the same. However, the correlations indicated that penetration rates are higher for lower GI values which may be attributed to the higher percentage of smaller and softer calcite/dolomite/carbonate grains in dolomite rocks. Higher GI values in pegmatites and leucogranites indicate a low penetration rate which could be due to higher percentage of harder minerals, i.e. feldspar and quartz grains which demand relatively higher stress to yield than that of dolomites. Moreover, in dolomite rocks, the grains are bound by a matrix indicating relatively soft rock characteristics aiding the drilling process. Whereas in pegmatite rocks, the crystals are tightly bound having an interlocking texture, indicating a hard rock characteristic that inhibits drilling.

The presence of ductile minerals such as mica in the rock specimen can also influence the drilling process. For example, frequent drill-bit jamming was observed during drilling tests in schist specimen (Figure 8). Near the top surface of the core, confinement levels are usually low, resulting in a rough cutting surface; however, at greater depths, the confinement increases leading to a smoother

drill-hole surface. These observations prove that petrographic characteristics influence drillability. Figure 9 presents the variation of DPR with GI across the tested rock variants. From the figure it can be observed that mean DPR values are directly proportional to mean GI values, except for primary rocks such as leucogranite and pegmatite, which might be attributed to the presence of harder minerals in such rocks. These results revealed that besides GI, mineral hardness also plays a vital role in altering rock drillability among the petrographic properties. Thus, GI was also accounted for in weighted mineral hardness (Mohs) values for various rocks and further correlated with mean DPR, as shown in Figure 10, which indicates an inverse relationship. Figure 11 shows the influence of MIS on DPR across the rock variants. Figure 12 presents the relationship between the proposed indices, MIS and GI corrected for mineral hardness (GIMHM).

From Figure 11, it can be observed that the MIS values for dolomite rocks are less than 60 while for siliceous dolomite rocks it varies between 40 and 60, with maximum values ranging from 90 to 100 for gneisses and schists. Overall, DPR is found to have a cubic relationship with MIS. From Figure 12, it can be observed that there exists a strong linear relationship between MIS and GIMHM, which indicates that as MIS values increases, GIMHM also increases. Figure 13 graphically depicts the change in DPR values across rock variants.

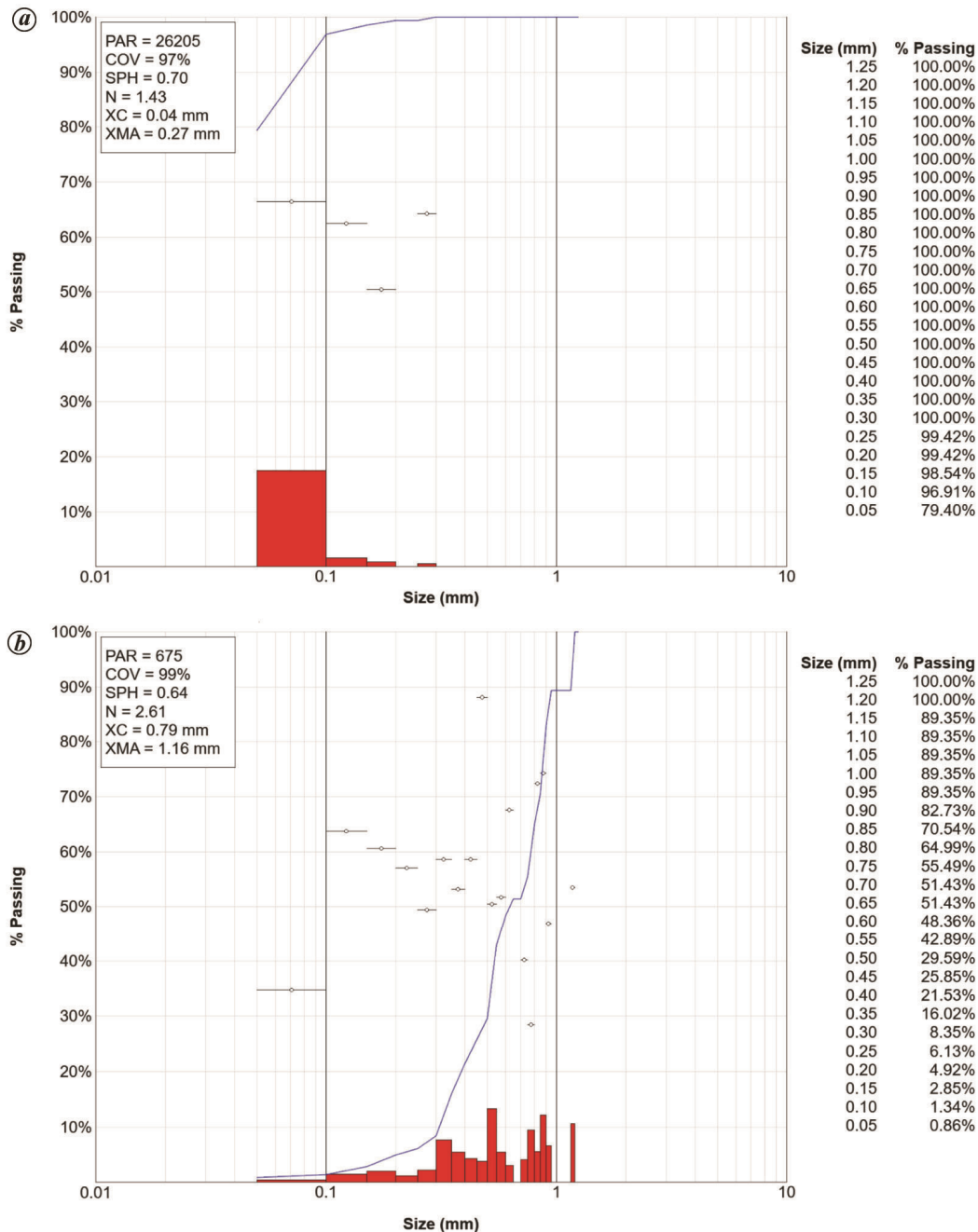


Figure 6. Grain size distribution curves for rocks with different GI values. *a*, GI = 126, DPR = 16 mm/min; *b*, GI = 1365, DPR = 3.1 mm/min.

Discussion

Among all the rock variants considered, pegmatite rock was found to have the largest grain size, while the characteristic grain size for the other variants was in the same range. Thus, the number of grains measured in pegmatite is least compared to that of dolomite, phyllite, schist and leucogranite with a rougher grain boundary. They were also found to be less circular than the other rock types, which introduces angularity of the grains. Thus, the aspect ratio increases in these rocks. Overall, pegmatites

have the largest geometrical parameter values like average mineral grain area, perimeter, length, breadth, elongation, GI and a more complex mineral assemblage compared to the other rock types resulting in a harder surface to drill; thus low drillability is observed.

Leucogranite, pegmatite and gneissic rocks were found to have a relatively higher N value than dolomite, phyllite and schist. Mean values of B were found to be similar for leucogranite and pegmatite, dolomite and phyllite, schist and gneiss. Siliceous dolomites were found to have the least B value probably due to the larger silica content and

therefore, they are observed to be more compact unlike rectangular leucogranites. Since the rocks considered in this study were mostly unaltered, all the grains were tightly packed resulting in almost uniform packing density. From the angle factor data, leucogranite and pegmatite

were found to have a larger number of grains with higher angles, i.e. oriented parallel to the drilling direction, while in schist the grains were found to be inclined.

Modal analysis and comparison of mineral content across rock types indicated that gneissic rocks contained

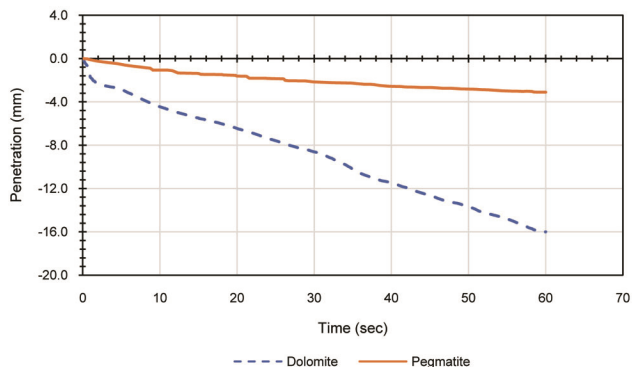


Figure 7. Penetration–time ($P-T$) curve for dolomite and pegmatite samples obtained from drilling tests.

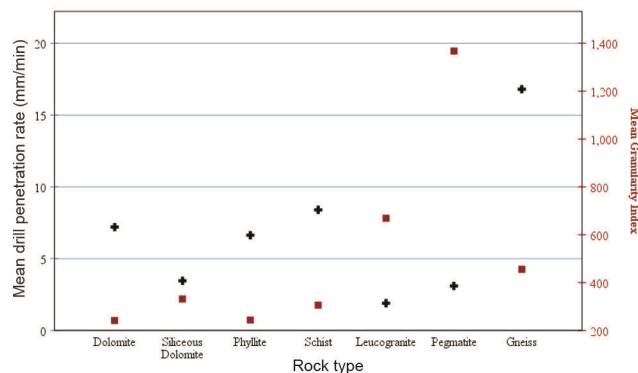
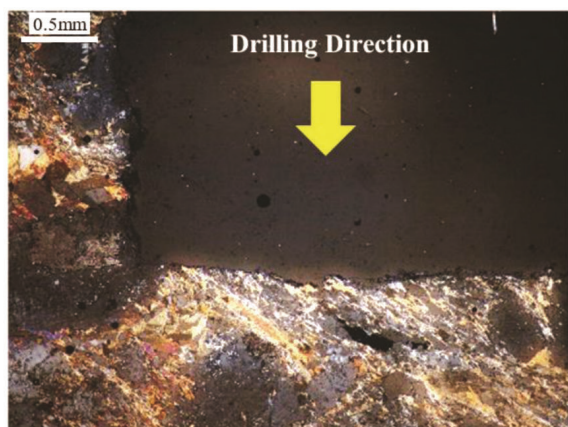
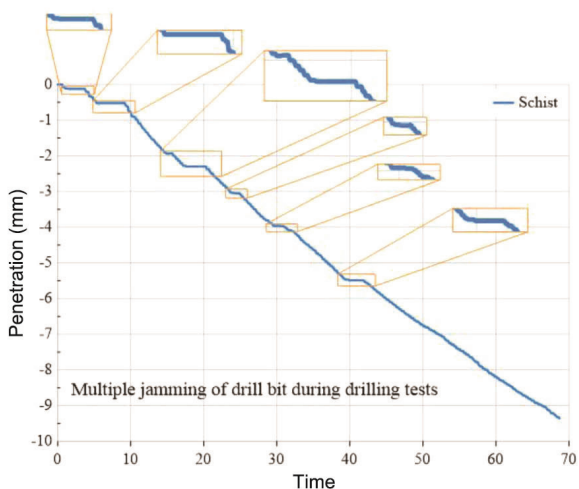


Figure 9. Variation of DPR with GI across rock types. +, Mean DPR, ■, Mean granularity index.



(a) Thin section of schist specimen



(b) Penetration–time curve of schist specimen

Figure 8. Bit jamming phenomenon observed in schistose rocks during drilling test.

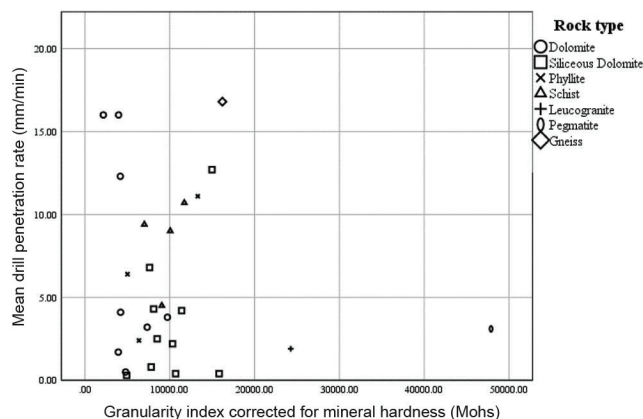


Figure 10. Variation of DPR with GI corrected for mineral hardness (Mohs) (GIMHM) across rock types.

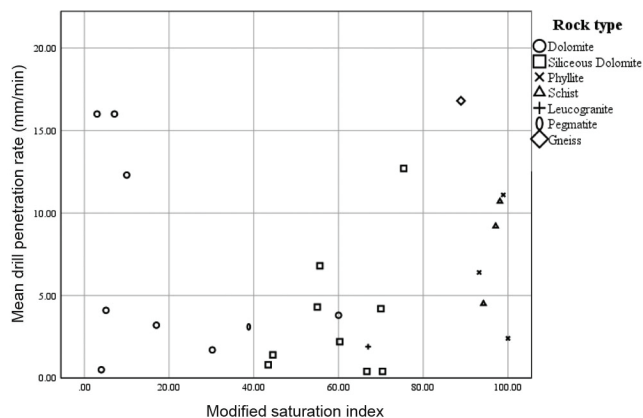


Figure 11. Variation of DPR with modified saturation index (MIS) across rock types.

maximum quartz content, while dolomite had the least. Due to their origin, maximum calcite/carbonate/dolomite content was observed in dolomite. The dolomite collected from Zawar being ore-bearing rocks was found to have opaque minerals in them. Pegmatite rocks contained maximum feldspar content, while schist contained maximum mica content. The dolomite was found to have homogeneous grain size distribution, while leucogranite rocks were found to be relatively less homogeneous. Phyllite, schist and gneiss were observed to have the largest MIS which might be due to the orientation of grains, while dolomite was found to have the least. This could also be due to the tight packing arrangement within dolomite grains.

Dolomite rocks being compact and tightly packed, the density and ultrasonic velocities were found to be higher than other rocks considered in this study. From the K_{IC} values, it was observed that dolomite, leucogranite and pegmatite were found to be tougher than schist or gneiss, probably due to the presence of oriented grains in schist or banded nature of gneissic rocks. Leucogranite, pegmatite and gneissic rocks were found to be relatively more abrasive, more brittle and had low tensile strength than dolomite, phyllite and schist. Pegmatite rocks were found

to have greater hardness, while phyllite, schist and gneiss had the least. DRI in siliceous dolomite was found to be least, while it was highest in gneiss. Siliceous dolomite was observed to have the highest UCS value and hence low DPR. Dolomite and pegmatite were found to have a higher modulus, thus offering more resistance by the rocks to deformation or strain under a given stress condition. While schist and phyllite were found to have low modulus, allowing larger strain. Phyllite was also seen to have a low Poisson's ratio. Gneissic rocks were observed to have the least cohesion, while dolomite and leucogranite had the most. Pegmatite had a higher friction angle due to rough grains. Phyllite was found to be more porous due to greater mica content in it. Rock drillability was found to be lower in siliceous dolomite and leucogranite, while gneissic rocks indicated better penetration rates. In the case of dolomite, the drilling rates were observed to have much variance due to the presence of hard and soft minerals in varying percentages. Figure 14 presents the PPM approach to determine rock drillability.

Conclusion

This pilot study primarily covered limited rock samples drilled under controlled conditions, reviewing the influence of various PPM properties on rock drillability. Analysis has revealed that no single property could explain the variance in drilling completely among all the studied petrographic features due to the complex mineral assemblage and varied grain hardness. Quartz content, MIS and

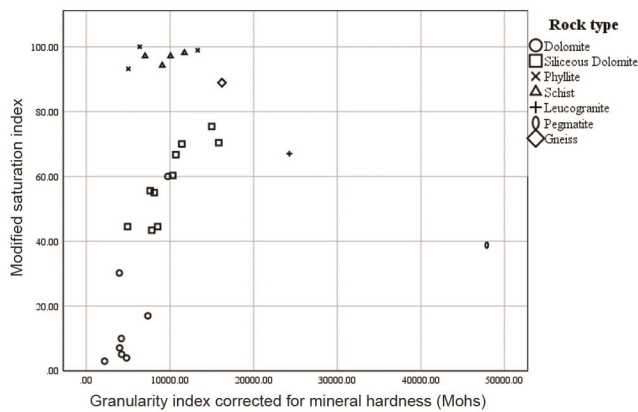


Figure 12. Relationship between modified saturation index and GIMHM.

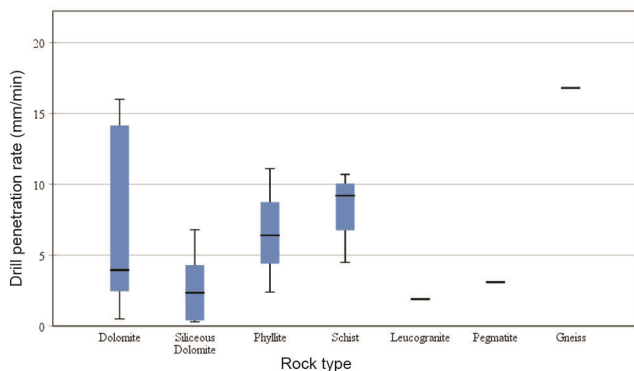


Figure 13. Box plot showing drill penetration rate for various rock types.

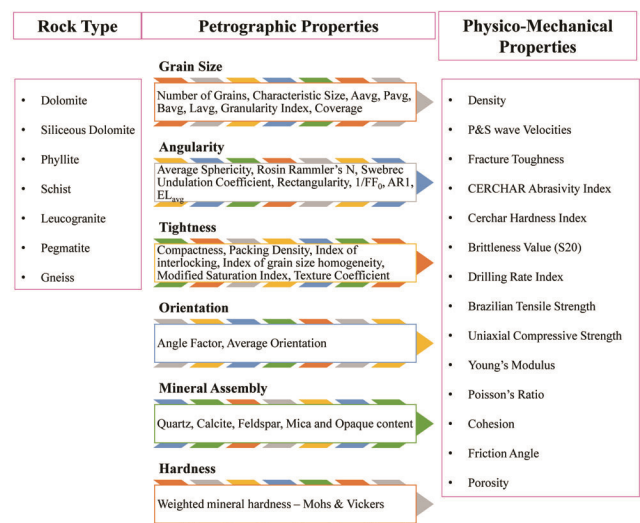
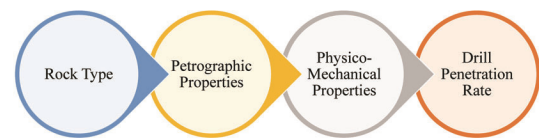


Figure 14. Petro-physico-mechanical approach to determine rock drillability.

calcite content were found to have a relatively higher correlation with DPR than other petrographic parameters. Quartz and calcite content in carbonate rocks altered DPR to a great extent. The developed GI corrected for mineral hardness was found to exhibit an interaction effect and showed a moderately inverse relationship with DPR. Advancements in digital imaging and processing techniques have led to a rapid estimation of GI and MSI, which further aids in DPR predictions. Among various physico-mechanical properties of the rocks studied, K_{IC} , CHI and UCS were found to influence rock drillability significantly, while BTS cohesion, porosity, modulus of elasticity, P -wave velocity and friction angle showed a moderate relationship with DPR. CAI, S -wave velocity, rock brittleness, Poisson's ratio and rock density did not strongly correlate with DPR. Both petrographic and physico-mechanical properties of the rocks were found to influence rock drillability; however, the latter could better explain the variability in drilling. With the incorporation of other rock variants, the proposed PPM approach can be further reinforced and extended to field applications.

1. Zare, S., Bruland, A. and Rostami, J., Evaluating D&B and TBM tunnelling using NTNU prediction models. *Tunn. Undergr. Space Technol.*, 2016, **59**, 55–64.
2. Bruland, A., *Hard Rock Tunnel Boring, Drillability Test Methods*, 1998, **8**, 1–22.
3. Barton, N., *TBM Tunnelling in Jointed and Faulted Rock*, A.A. Balkema, Rotterdam, The Netherlands, 2000.
4. Siva Prasad, B. N. V. and Murthy, V. M. S. R., Laboratory investigations into fracture propagation characteristics of rock material. *AIP Conf. Proc.*, 2018, 020009-1–7.
5. Siva Prasad, B. N. V. and Murthy, V. M. S. R., Influence of rock abrasivity and bit wear on drill penetration rate. In *INDOROCK: 7th Indian Rock Conference*, New Delhi, India, 2017, pp. 387–395.
6. Yetkin, M. E., Examining of rock drilling properties in underground metal mine excavation. *An. Acad. Bras. Cienc.*, 2021, **93**, 1–10.
7. Piri, M., Mikaeil, R., Hashemolhosseini, H., Baghbanan, A. and Ataei, M., Study of the effect of drill bits hardness, drilling machine operating parameters and rock mechanical parameters on noise level in hard rock drilling process. *Meas. J. Int. Meas. Confed.*, 2021, **167**, 108447.
8. Inanloo Arabi Shad, H., Sereshki, F., Ataei, M. and Karamoozian, M., Prediction of rotary drilling penetration rate in iron ore oxides using rock engineering system. *Int. J. Min. Sci. Technol.*, 2018, **28**, 407–413.
9. Li, Y., She, L., Wen, L. and Zhang, Q., Sensitivity analysis of drilling parameters in rock rotary drilling process based on orthogonal test method. *Eng. Geol.*, 2020, **270**, 1–9.
10. Thuro, K. and Plinninger, R. J., Hard rock tunnel boring, cutting, drilling and blasting: rock parameters for excavatability. In *10th ISRM Congress*, Seattle, 2003, pp. 1–7.
11. Rostami, J., Ozdemir, L., Bruland, A. and Dahl, F., Review of issues related to Cerchar abrasivity testing and their implications on geotechnical investigations and cutter cost estimates. In *Proceedings of the Rapid Excavation and Tunnelling Conference*, Seattle, 2005, pp. 738–751.
12. Thuro, K., Drillability prediction: geological influences in hard rock drill and blast tunnelling. *Geol. Rundsch.*, 1997, **86**, 426–438.
13. Dahl, F., Grov, E. and Breivik, T., Development of a new direct test method for estimating cutter life, based on the Sievers' J miniature drill test. *Tunn. Undergr. Space Technol.*, 2007, **22**, 106–116.
14. Villeneuve, M. C., Examination of geological influence on machine excavation of highly stressed tunnels in massive hard rock. Ph.D. thesis, Queen's University, 2008.
15. Zare, S., Prediction model and simulation tool for time and costs of drill and blast tunnelling. NTNU, Trondheim, Norway, 2007.
16. Zhao, K., Janutolo, M. and Barla, G., A completely 3D model for the simulation of mechanized tunnel excavation. *Rock Mech. Rock Eng.*, 2012, **45**, 475–497.
17. Siva Prasad, B. N. V., Murthy, V. M. S. R. and Pandey, S. K., Investigations on rock drillability applied to underground mine development vis-à-vis drill selection. In *Recent Advances in Rock Engineering*, Atlantis Press, Bengaluru, India, 2016, pp. 399–403.
18. MacKenzie, W., Adams, A. and Brodie, K., *Rocks and Minerals in Thin Section*, CRC Press, Balkema, 2017, 2nd edn.
19. Howarth, D. F., The effect of pre-existing microcavities on mechanical rock performance in sedimentary and crystalline rocks. *Int. J. Rock Mech. Min. Sci.*, 1987, **24**, 223–233.
20. Howarth, D. F., Adamson, W. R. and Berndt, J. R., Correlation of model tunnel boring and drilling machine performances with rock properties. *Int. J. Rock Mech. Min. Sci. Geomech. Abstr.*, 1986, **23**, 171–175.
21. Howarth, D. F. and Rowlands, J. C., Quantitative assessment of rock texture and correlation with drillability and strength properties. *Rock Mech. Rock Eng.*, 1987, **20**, 57–85.
22. Singh, T. N., Jain, A. and Sarkar, K., Petrophysical parameters affecting the microbit drillability of rock. *Int. J. Min. Miner. Eng.*, 2009, **1**, 261–277.
23. Sandvik Tamrock Corp., *Rock Excavation Handbook*, 1999.
24. Jain, R., Presence of base metals in the southern extension of Zawarmala dolomite, Udaipur, Rajasthan, India. *Curr. Sci.*, 2021, **121**, 962–966.
25. <http://www.portergeo.com.au/database/mineinfo.asp?mineid=mn296> (accessed on 9 January 2022).
26. Roy, A. B., Evolution of the Precambrian crust of the Aravalli Mountain Range. In *Developments in Precambrian Geology*, 1990, pp. 327–347.
27. Siva Prasad, B. N. V., Thapliyal, A. P., Bhusan, R. and Naik, S. R., Delineation of cavity in downstream surge chamber at Punatsangchhu-II Hydroelectric Project, Bhutan. *J. Geol. Res.*, 2019, **1**, 5–11.
28. GSI, *Geological Map of India*, Geological Survey of India, Kolkata, 8 January 2022.
29. Long, S., McQuarrie, N., Tobgay, T., Grujic, D. and Hollister, L., Geologic map of Bhutan. *J. Maps*, 2011, **7**, 184–192.
30. Paone, J., Madson, D. and Bruce, W. E., *Drillability Studies – Laboratory Percussive Drilling Oxford University*, United States Department of the Interior, Bureau of Mines, 1969.
31. Tandanand, S. and Unger, H. F., Drillability determination – a drillability index for percussive drills. US Department of the Interior, Bureau of Mines, 1975.
32. Rabia, H., A unified prediction model for percussive and rotary drilling. *Min. Sci. Technol.*, 1985, **2**, 207–216.
33. Olsson, W. A., Grain size dependence of yield stress in marble. *J. Geophys. Res.*, 1974, **79**, 4859–4862.
34. Tandon, R. S. and Gupta, V., The control of mineral constituents and textural characteristics on the petrophysical & mechanical (PM) properties of different rocks of the Himalaya. *Eng. Geol.*, 2013, **153**, 125–143.
35. Ajalloeian, R., Mansouri, H. and Baradaran, E., Some carbonate rock texture effects on mechanical behavior, based on Koohrang tunnel data, Iran. *Bull. Eng. Geol. Environ.*, 2017, **76**, 295–307.
36. Hugman, R. H. and Friedman, M., Effects of texture and composition on mechanical behaviour of experimentally deformed carbonate rock. *Am. Assoc. Pet. Geol. Bull.*, 1979, **63**, 1478–1489.

37. Onodera, T. F. and Asoka Kumara, H. M., Relation between texture and mechanical properties of crystalline rocks. *Bull. Int. Assoc. Eng. Geol.*, 1980, **22**, 173–177.
38. Bell, F. G. and Culshaw, M. G., Petrographic and engineering properties of sandstones from the Sneinton Formation, Nottinghamshire, England. *Q. J. Eng. Geol.*, 1998, **31**, 5–19.
39. Ulusay, R., Türeli, K. and Ider, M. H., Prediction of engineering properties of a selected litharenite sandstone from its petrographic characteristics using correlation and multivariate statistical techniques. *Eng. Geol.*, 1994, **38**, 135–157.
40. Ersoy, A. and Waller, M. D., Textural characterisation of rocks. *Eng. Geol.*, 1995, **39**, 123–136.
41. Yusof, N. Q. A. M. and Zabidi, H., Correlation of mineralogical and textural characteristics with engineering properties of granitic rock from Hulu Langat, Selangor. *Procedia Chem.*, 2016, **19**, 975–980.
42. Pfikryl, R., Assessment of rock geomechanical quality by quantitative rock fabric coefficients: limitations and possible source of misinterpretations. *Eng. Geol.*, 2006, **87**, 149–162.
43. Ehrlich, R. and Chin, M., Fourier grain-shape analysis: a new tool for sourcing and tracking abyssal silts. *Mar. Geol.*, 1980, **38**, 219–231.
44. Mazzullo, J. and Crisp, J. A., Quartz-grain shape: a record of the source of fine-grained sediments. *Geo-Marine Lett.*, 1984, **4**, 197–202.
45. Smorodinov, M. I., Motovilov, E. A. and Volkov, V. A., Determination of correlation relationships between strength and some physical characteristics of rocks. In Second Congress, International Society for Rock Mechanics, Belgrade, 1970, pp. 35–37.
46. Bieniawski, Z. T., Mechanism of brittle fracture of rock. Part I – Theory of the fracture process. *Int. J. Rock Mech. Min. Sci.*, 1967, **4**, 395–406.
47. Sprunt, E. S. and Brace, W. F., Direct observation of microcavities in crystalline rocks. *Int. J. Rock Mech. Min. Sci.*, 1974, **11**, 139–150.
48. Williams, H., Turner, F. J. and Gilbert, C. M., *Petrography: An Introduction to the Study of Rocks in Thin Section*, W.H. Freeman, San Francisco, USA, 1954.
49. Suggested method for petrographic description of rocks. *Int. Soc. Rock Mech.*, 1978, **8**, 43–45.
50. Lindqvist, J. and Åkesson, U., Image analysis applied to engineering geology, a literature review. *Bull. Eng. Geol. Environ.*, 2001, **60**, 117–122.
51. Su, C., Xu, S. J., Zhu, K. Y. and Zhang, X. C., Rock classification in petrographic thin section images based on concatenated convolutional neural networks. *Earth Sci. Informatics*, 2020, **13**, 1477–1484.
52. Reedy, C. L., Review of digital image analysis of petrographic thin sections in conservation research. *J. Am. Inst. Conserv.*, 2006, **45**, 127–146.
53. Rubo, R. A., Carneiro, C. de C., Michelin, M. F. and Gioria, R. dos S., Digital petrography: mineralogy and porosity identification using machine learning algorithms in petrographic thin section images. *J. Pet. Sci. Eng.*, 2019, **183**, 1–14.
54. Reedy, C. L., Anderson, J., Reedy, T. J. and Liu, Y., Image analysis in quantitative particle studies of archaeological ceramic thin sections. *Adv. Archaeol. Pract.*, 2014, **2**, 252–268.
55. Wipware Inc, *Sampling and Analysis Guide*, 2013, pp. 1–39.
56. Aligholi, S., Lashkaripour, G. R., Ghafoori, M. and Azali, S. T., Evaluating the relationships between NTNU/SINTEF drillability indices with index properties and petrographic data of hard igneous rocks. *Rock Mech. Rock Eng.*, 2017, **50**, 2929–2953.
57. Field, A., *Discovering Statistics using IBM SPSS Statistics*, SAGE Publications, 2018, 5th edn.

ACKNOWLEDGEMENTS. We thank the Director, NIRM, Bengaluru Hindustan Zinc Limited (HZL) management and project authorities for providing resources to perform this study. We also thank the Rock Excavation and Rock Mechanics Laboratories, Department of Mining Engineering, IIT(ISM), Dhanbad, and Dr Rabi Bhusan (NIRM) and Dr Prabodha Ranjan Sahoo (IIT(ISM), Dhanbad) help for petrographic assessment. This study is part of the Ph.D. work of the B.N.V.S.P. at IIT(ISM), Dhanbad.

Received 13 October 2021; revised accepted 5 February 2022

doi: 10.18520/cs/v122/i8/907-917